has identified a strong proton acceptor (Asp-235) near the axial imidazole ring NH, which, due to sequence homology in this region between CcP[28] and HRP,[29] is likely similarly situated in resting-state HRP, as depicted in Figure 1E. Since resting-state HRP is five-coordinate,[12] we assume the characteristic domed porphyrin and a sizable out-of-plane displacement of the iron[25] such that the imidazole ring NH can interact with the carboxylate. Upon coordination of cyanide, the conversion to low-spin iron flattens the porphyrin and brings the iron into the plane.[25] Because of the tight clamping of the heme periphery,[30] this resulting 0.5–1.0-Å movement of the imidazole ring breaks the salt bridge to the amino acid, with the proton retained by the carboxylate rather than the imidazole ring, as depicted in Figure 1F. Thus the six-coordinate compounds I and II, but not five-coordinate resting-state HRP, may possess the axial imidazolate to stabilize the higher oxidation state of iron.

Nuclear Overhauser effect studies of the rapidly exchanging peaks a and b of HRPCN in H_2O (not shown) reveal that the two peaks are in spatial proximity and are consistent with arising from a histidine in the distal environment of the heme, for which strong interaction with a coordinated ligand has been demonstrated by IR spectroscopy.[31] Further definitive assignments of the labile proton signals are in progress.

(26) Poulos, T. L.; Kraut, J. *J. Biol. Chem.* **1980**, *255*, 8199–8205.
(27) Finzel, B. C.; Poulos, T. L.; Kraut, J. *J. Biol. Chem.* **1984**, *259*, 13027–13036.
(28) Takio, K.; Titani, K.; Ericsson, L. H.; Yonetani, T. *Arch. Biochem. Biophys.* **1980**, *203*, 615–629.
(29) Welinder, K. G. *Eur. J. Biochem.* **1979**, *96*, 483–502.
(30) La Mar, G. N.; de Ropp, J. S.; Smith, K. M.; Langry, K. C. *J. Am. Chem. Soc.* **1983**, *105*, 4576–4580.
(31) Smith, M. L.; Ohlsson, P.-I.; Paul, K. G. *FEBS Lett.* **1983**, *163*, 303–305.

Metal–Metal Bonds Involving Actinides. Synthesis and Characterization of a Complex Having an Unsupported Actinide to Transition-Metal Bond

Richard S. Sternal, Carolyn P. Brock, and Tobin J. Marks*

*Department of Chemistry, Northwestern University
Evanston, Illinois 60201*

Received August 22, 1985

While metal–metal bonding is a ubiquitous feature of transition-metal chemistry and heterobimetallic ("early–late") systems are of considerable current interest,[1,2] no well-characterized example of an actinide to transition-metal bond unsupported/un-

(1) (a) Edidin, R. T.; Longato, B.; Martin, B. D.; Matchett, S. A.; Norton, J. R. In "Organometallic Compounds"; Shapiro, B. L.; Ed.; Texas A&M University Press: College Station, TX, 1983; pp 260–280 and references therein. (b) Roberts, D. A.; Geoffroy, G. L. In "Comprehensive Organometallic Chemistry"; Wilkinson, G.; Stone, F. G. A.; Abel, E. W., Eds.; Pergamon Press: Oxford, 1982; Vol. 6, Chapter 40. (c) Masters, C. *Adv. Organomet. Chem.* **1979**, *17*, 61–103.
(2) (a) Casey, C. P.; Jordon, R. F.; Rheingold, A. L. *J. Am. Chem. Soc.* **1983**, *105*, 665–667. (b) Casey, C. P.; Jordon, R. F.; Rheingold, A. L. *Organometallics* **1984**, *3*, 504–506. (c) Casey, C. P.; Palermo, R. E.; Jordon, R. F.; Rheingold, A. L. *J. Am. Chem. Soc.* **1985**, *107*, 4597–4599. (d) Sartain, W. J.; Selegue, J. P. *J. Am. Chem. Soc.* **1985**, *107*, 5818–5820. (e) Barger, P. T.; Bercaw, J. E. *Organometallics* **1984**, *3*, 278–284.
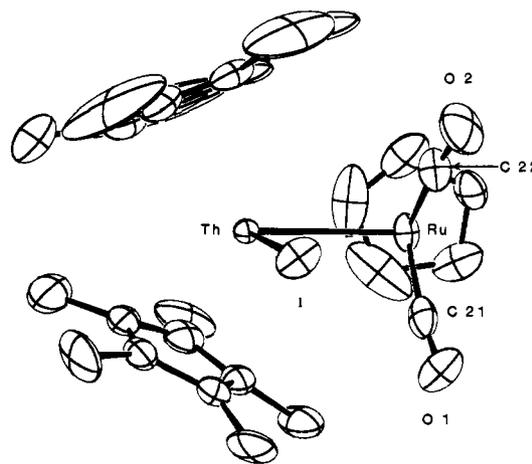
Figure 1. Perspective drawing of the molecular structure of Cp'₂Th(I)-Ru(Cp)(CO)₂ (2). The shapes of the ellipsoids correspond to 50% probability contours of atomic displacement. Individual bond lengths (Å) and angles (deg) of interest: Th–Ru, 3.0277 (6); Th–I, 3.0435 (6); Th–C (Cp' ring), 2.82 (1, 2, 4, 10);[13b] Ru–C21, 1.88 (2); Ru–C22, 1.84 (1); Ru–C(Cp ring), 2.29 (1, 1, 2, 5);[13b] Th–Ru–C21, 83.8 (2); Th–Ru–C22, 84.4 (3); C21–Ru–C22, 88.3 (5); Th–Ru–Cp centroid, 118.4.

complicated by bridging ligands[3] exists. The competing formation of isocarbonyl linkages (A)[1a,4] between highly oxophilic 5f centers[5]

$$\underset{\text{A}}{\overset{+}{An}\leftarrow O\equiv C - \overline{M}L_n} \quad vs \quad \underset{\text{B}}{An - \overset{\overset{O}{\overset{|||}{C}}}{\underset{\downarrow}{}}ML_n}$$

An = actinide; M = transition metal
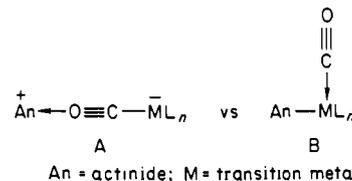
and metal carbonyl synthons has been a major obstacle,[6] and in our view, strategies to promote B must minimize crowding around the An–MLₙ(CO) bond and/or provide an MLₙ(CO) fragment with an appropriately directed, high-lying, metal-centered HOMO. Using MLₙ(CO) = CpRu(CO)₂[2a–d,7] and An = Cp'₂Th(X) (Cp = η^5-C₅H₅; Cp' = η^5-(CH₃)₅C₅) as prototypes in this strategy, we report the synthesis and structural characterization of the first complexes with *direct, unsupported*, actinide to transition-metal bonds.

The reaction of Cp'₂ThX₂ (X = Cl,[8] I[9]) with CpRu(CO)₂Na[10]

(3) In phosphido-bridged systems, relatively close actinide–transition-metal contacts are thought to reflect some degree of transition-metal → thorium dative bonding: (a) Ritchey, J. M.; Zozulin, A. J.; Wrobleski, D. A.; Ryan, R. R.; Wasserman, H. J.; Moody, D. C.; Paine, R. T. *J. Am. Chem. Soc.* **1985**, *107*, 501–503. (b) Hay, P. J.; Ryan, R. R.; Salazar, K. V.; Wrobleski, D. A.; Sattelberger, A. P. *J. Am. Chem. Soc.*, submitted for publication. (c) Ortiz, J. V., submitted for publication. We thank these authors for preprints.
(4) (a) Darensbourg, M. Y. *Prog. Inorg. Chem.* **1985**, *33*, 221–274. (b) Horwitz, C. P.; Shriver, D. F. *Adv. Organomet. Chem.* **1984**, *23*, 219–305. (c) Boncella, J. M.; Andersen, R. A. *Inorg. Chem.* **1984**, *23*, 432–437 and references therein. (d) Merola, J. S.; Campo, K. S.; Gentile, R. A.; Modrick, M. A.; Zentz, S. *Organometallics* **1984**, *3*, 334–337 and references therein. (e) Marsella, J. A.; Huffman, J. C.; Caulton, K. G.; Longato, B.; Norton, J. R. *J. Am. Chem. Soc.* **1982**, *104*, 6360–6368 and references therein. (f) Hamilton, D. M., Jr.; Willis, W. S.; Stucky, G. D. *J. Am. Chem. Soc.* **1981**, *103*, 4255–4256. (g) Onaka, S.; Furuichi, N. *J. Organomet. Chem.* **1979**, *173*, 77–88. (h) Crease, A. E.; Legzdins, P. *J. Chem. Soc., Dalton Trans.* **1973**, 1501–1507.
(5) (a) Marks, T. J.; Fragalà, I. L., Eds. "Fundamental and Technological Aspects of Organo-f-Element Chemistry"; Reidel: Dordrecht 1985. (b) Marks, T. J.; Ernst, R. D. In ref 1b, Vol. 3, Chapter 21.
(6) (a) Marks, T. J., unpublished results. (b) Bennett, R. L.; Bruce, M. I.; Stone, F. G. A. *J. Organomet. Chem.* **1971**, *26*, 355–356. (c) Fagan, P. J.; Mintz, E. A.; Marks, T. J., unpublished results on Cp₂U[Mo(Cp(CO)₃]₂ quoted in ref 5b, p 261. (d) Dormand, A.; Moise, C. *Polyhedron* **1985**, *4*, 595–598.
(7) Electronic structure studies on related fragments: (a) Bursten, B. E.; Gatter, M. G. *J. Am. Chem. Soc.* **1984**, *106*, 2554–2558. (b) Schilling, B. E. R.; Hoffmann, R.; Lichtenberger, D. L. *J. Am. Chem. Soc.* **1979**, *101*, 585–591.
(8) Fagan, P. J.; Manriquez, J. M.; Maatta, E. A.; Seyam, A. M.; Marks, T. J. *J. Am. Chem. Soc.* **1981**, *103*, 6650–6667.

Communications to the Editor

J. Am. Chem. Soc., Vol. 107, No. 26, 1985 8271

proceeds according to eq 1. Initial attempts using larger Ru/Th

$$\text{Cp}'_2\text{ThX}_2 + \text{CpRu(CO)}_2\text{Na} \xrightarrow[\text{25 °C, 12 h}]{\text{THF}}$$
$$\text{Cp}'_2\text{Th(X)Ru(Cp)(CO)}_2 + \text{NaX} \quad (1)$$
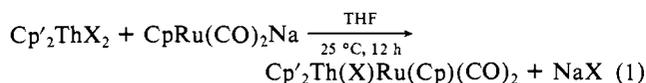
1, X = Cl, colorless needles, 50% isolated yield

2, X = I, pale yellow needles, 50% isolated yield

ratios have not led to multiple substitution under these conditions. Sparingly soluble, exceedingly air-sensitive complexes **1** and **2** can be recrystallized from toluene/pentane and characterized by standard analytical/spectroscopic methodology.[11] Solid-state and hydrocarbon solution infrared spectra give no evidence of an isocarbonyl[4,6] and ν_{CO} frequencies in heptane, (**1**, 2033 s, 1973 s cm^{-1}; **2**, 2033 s, 1973 s cm^{-1}) are typical of CpRu(CO)$_2$X species where X is approximately as electron withdrawing as an alkyl group,[12a,b] more so than a SiMe$_3$ or GeMe$_3$[12c] but less so than a fluorocarbon[12d] or halogen.[12a] Chlorine/iodine electronic differences are apparently not transmitted to the ruthenium center. Infrared spectra in THF solution are similar (**1**, 2025 s, 1959 s cm^{-1}; **2**, 2023 s, 1959 s cm^{-1}).

Crystals of **2** suitable for X-ray diffraction[13a] were grown by diffusion of pentane into a toluene solution of **2**. The thorium coordination geometry (Figure 1)[13b] is of the Cp$'_2$Th(X)Y type and is unexceptional[5,14] ($\angle$Cp' centroid–Th–Cp' centroid = 128.8°; $\angle$X–Th–Y = 94.96 (2)°) except for the presence of a Th–Ru bond of length 3.0277 (6) Å. This contact can be compared to calculated Th–Ru distances of ca. 3.14 Å from metallic radii,[15] ca. 3.23 Å from homobimetallic Ru–Ru[16] and Th–Th[17] compounds, ca. 3.12–3.16 Å from Zr–Ru compounds[2a–c] corrected for the Th(IV) ionic radius,[18] and observed distances of ca. 2.87–3.24

(9) From (Cp$'_2$ThH$_2$)$_2$[8] and CH$_3$I (Moloy, K. G., unpublished results).

(10) Gibson, D. H.; Hsu, W.-L.; Ahmed, F. U. *J. Organometal. Chem.* **1981**, *215*, 379–401.

(11) (a) **1**: ^{1}H NMR (C$_6$D$_6$, 30 °C) δ 4.78 (s, 5 H, CpRu), 2.07 (s, 30 H, Cp$'_2$Th); ^{13}C{^{1}H} NMR (C$_6$D$_5$CD$_3$, –25 °C) δ 204.9 (CO), 85.15 (Cp), 12.73 (Cp'–CH$_3$), the Cp'–C signal is obscured by the solvent. Anal. Calcd. for C$_{27}$H$_{35}$ThRuClO$_2$: C, 42.66; H, 4.64; Cl, 4.66. Found: C, 41.66; H, 4.90; Cl, 4.29. (b) **2**: ^{1}H NMR (C$_6$D$_6$, 30 °C) 4.74 (s, 5 H, CpRu), 2.14 (s, 30 H, Cp$'_2$Th); ^{13}C{^{1}H} NMR (C$_6$D$_5$CD$_3$, –25 °C) δ 204.5 (CO), 85.21 (Cp), 13.68 (Cp'–CH$_3$), the Cp'C signal is obscured by the solvent. Anal. Calcd. for C$_{27}$H$_{35}$ThRuIO$_2$: C, 38.08; H, 4.14. Found: C, 38.21; H, 4.17.

(12) (a) Davison, A.; McCleverty, J. A.; Wilkinson, G. *J. Chem. Soc.* **1963**, 1133–1138. (b) Cotton, F. A.; Marks, T. J. *J. Am. Chem. Soc.* **1969**, *91*, 7523–7524. (c) Sosinsky, B. A.; Knox, S. A. R.; Stone, F. G. A. *J. Chem. Soc., Dalton Trans.* **1975**, 1633–1640. (c) Blackmore, T.; Bruce, M. I.; Stone, F. G. A. *J. Chem. Soc. A* **1968**, 2158–2162.

(13) (a) The compound crystallizes in the monoclinic space group $P2_1/n$ (an alternate setting of No. 14, $P2_1/c$) with a = 11.758 (2) Å, b = 15.586 (2) Å, c = 14.667 (3) Å, β = 92.29 (2)°, and Z = 4 at 163 (2) K. The structure was refined (full-matrix least squares) to agreement factors R and R_w on F_o of 0.039 and 0.046 with 289 variables and the 4484 reflections having $F_o{}^2 \geq 3\sigma(F_o{}^2)$ out of the 6427 unique data measured with an Enraf-Nonius CAD4 diffractometer using Mo Kα radiation (λ = 0.70173 Å; $2\theta_{max}$ = 55°). A full description of the structure determination and a discussion of the Cp' disorder suggested by the elongated thermal ellipsoids in Figure 1 are included with the supplementary material. (b) The first number in parentheses following an averaged value of a bond length or angle is the estimated standard deviation of an individual datum. The second and third numbers are the average and maximum deviations from the averaged value, respectively. The fourth number represents the number of individual measurements that are included in the average value.

(14) (a) Marks, T. J.; Day, V. W. In ref 5a, pp 115–193. (b) Bruno, J. W.; Smith, G. M.; Marks, T. J.; Fair, C. K.; Schultz, A. J.; Williams, J. W. *J. Am. Chem. Soc.*, in press. (c) Bruno, J. W.; Marks, T. J.; Day, V. W. *J. Organomet. Chem.* **1983**, *250*, 237–246. (d) Marks, T. J.; Manriquez, J. M.; Fagan, P. J.; Day, V. W.; Day, C. S.; Vollmer, S. H. *ACS Symp. Ser.* **1980**, *131*, 1–29.

(15) Wells, A. F. "Structural Inorganic Chemistry", 5th ed.; Clarendon Press: Oxford, 1984; pp 1286–1288.

(16) (a) Vollhardt, K. P. C.; Weidman, T. W. *J. Am. Chem. Soc.* **1983**, *105*, 1676–1677 (2.821 (1) Å). (b) Behrens, U.; Weiss, E. *J. Organomet. Chem.* **1975**, *96*, 435–450 (2.845 (1) Å).

(17) (a) The closest Th–Th contact in a molecular compound is 3.628 (2) Å in Me$_2$Si(Me$_4$C$_5$)$_2$Th(μ-H)$_4$Th(Me$_4$C$_5$)SiMe$_2$: Fendrick, C. M.; Day, V. W.; Marks, T. J., submitted for publication. Fendrick, C. M., Ph.D. Thesis, Northwestern University, June 1985. (b) A similar thorium radius is obtained using Th–C (σ) distances from Cp$'_2$Th(alkyl)$_2$ compounds.

(18) Shannon, R. D. *Acta Crystallogr., A* **1976**, *A32*, 751–767.

Å in ThRu intermetallics.[19] The Th–Ru distance in **2** is among the shortest of these values. The "piano stool" ruthenium coordination geometry (Figure 1) is metrically typical of CpRu(CO)$_2$X molecules,[2,20] and there is no significant interaction between the thorium atom and the carbonyl ligands (Th–C 3.39 (1), 3.39 (1) Å; Th–O = 4.11 (1), 4.14 (1) Å). Judging from the spectroscopic data, it is likely that the structure of **1** is very similar to that of **2**.

Viewed schematically along the Ru–Th vector, it can be seen that in the solid state, **2** adopts one of two possible conformations (C, as opposed to enantiomorphous D and E).[12b] While C may
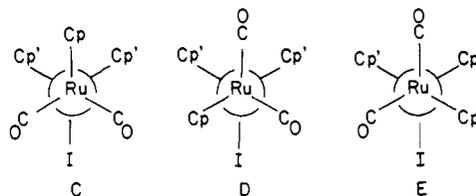
optimize interactions between Cp$'_2$Th(I)$^+$ σ-bonding MO's[21] in the equatorial girdle and the CpRu(CO)$_2^-$ HOMO[7] in the plane bisecting $\angle$C21–Ru–C22, it may also minimize nonbonded repulsions. Regarding the possible presence of D,E, variable-temperature ^{1}H and ^{13}C NMR spectra of **2** reveal the presence of two species at low temperature which are in dynamic equilibrium at room temperature ($T_c \sim$ +20 °C). The isomer ratio in THF-d_8 (–60 °C) is $\sim$1.4:1 with the former having magnetically equivalent Ru–^{13}CO ligands (δ 206.0, presumably C) and the latter, nonequivalent ligands (δ 226.5, 214.0 of equal intensity, presumably D,E).[22a] Results in C$_6$D$_5$CD$_3$ are qualitatively similar, although the ratio of isomers is $\sim$15:1 (–60 °C).[22b] Futher studies of this equilibrium are in progress.

In regard to the reactivity of the Th–Ru bond, the infrared spectra in THF indicate that heterolysis[1a,23,24] is not favorable (eq 2). However, we find *tert*-butanolysis of **2** to CpRu(CO)$_2$H

$$\text{Cp}'_2\text{Th(I)Ru(Cp)(CO)}_2 + n\text{THF} \rightleftharpoons$$
$$\text{Cp}'_2\text{Th}^+\text{(I)·THF}_n + \text{CpRu(CO)}_2^- \quad (2)$$
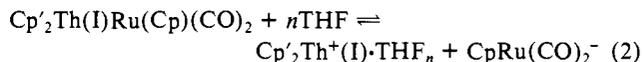
(identified by NMR[12a]) and the corresponding thorium alkoxide[25] (eq 3) to be rapid and reaction also to occur with H$_2$ and CO (the

$$\text{Cp}'_2\text{Th(I)RuCp(CO)}_2 + t\text{-BuOH} \rightarrow$$
$$\text{Cp}'_2\text{Th(I)(O-}t\text{-Bu)} + \text{CpRu(CO)}_2\text{H} \quad (3)$$

nature of these products is under investigation).

These results demonstrate that complexes having unsupported actinide to transition–metal bonds are synthetically accessible. Future efforts will explore the range of 5f, 4f, bimetallics that can be synthesized and their structures, thermochemistry, and reactivity.

(19) (a) Pearson, W. B., Ed. "Structure Reports"; Oosthoek: Utrecht, 1961; Vol. 26, pp 236–237. (b) *Ibid.* 1962; Vol. 27, p 367. (c) Thomson, J. R. *Nature (London)* **1962**, *194*, 465. (d) Thomson, J. R. *J. Less-Common Met.* **1963**, *5*, 437–442.

(20) (a) Lin, Y. C.; Calabrese, J. C.; Wreford, S. S. *J. Am. Chem. Soc.* **1983**, *105*, 1679–1680. (b) Adams, H.; Bailey, N. A.; White, C. *Inorg. Chem.* **1983**, *22*, 1155–1158. (c) Wagner, H.; Jungbauer, A.; Thiele, G.; Behrens, H. *Z. Naturforsch., B* **1979**, *34B*, 1487–1490.

(21) (a) Ortiz, J. V.; Hoffmann, R. *Inorg. Chem.* **1985**, *24*, 2095–2104 (Cp$_2$Ln fragments). (b) Saillard, J. Y., private communication (Cp$_2$Ln fragments). (c) Lauher, J. W.; Hoffmann, R. *J. Am. Chem. Soc.* **1976**, *98*, 1729–1742.

(22) (a) All expected magnetic nonequivalences are resolved except Cp',Cp' within D,E. (b) The predominant isomer has magnetically equivalent Cp' and CO ligands, suggestive of C.

(23) (a) Ernst, R. D.; Marks, T. J. *Inorg. Chem.* **1978**, *17*, 1477–1484. (b) Ernst, R. D.; Marks, T. J.; Ibers, J. A. *J. Am. Chem. Soc.* **1977**, *99*, 2098–2107. (c) Ernst, R. D.; Marks, T. J.; Ibers, J. A. *J. am. Chem. Soc.* **1977**, *99*, 2090–2098.

(24) CpRu(CO)$_2$Na in THF: ν_{CO} = 1904 s, 1825 s, cm^{-1}.

(25) An authentic sample was prepared by standard procedures[8] from Cp$'_2$ThI$_2$ + KO-t-Bu. ^{1}H NMR (C$_6$D$_6$) δ 1.27 (s, 9 H), 2.10 (s, 30 H).

Supplementary Material Available: Experimental details including description of disorder problem, positional and anisotropic displacement parameters, bond lengths and angles, and observed and calculated structure-factor amplitudes (61 pages). Ordering information is given on any current masthead page.

Spectral and Electrochemical Identification of Iron(IV)–Oxo Porphyrin and Iron(IV)–Oxo Porphyrin π-Cation Species

Thomas S. Calderwood, William A. Lee, and
Thomas C. Bruice*

*Department of Chemistry, University of California at
Santa Barbara, Santa Barbara, California 93106*

Received July 30, 1985

Iron(IV) protoporphyrin IX species have been shown or proposed to play important roles in the mechanisms of peroxidase, cytochrome P-450, and cytochrome oxidase enzymes.[1] Studies focused on the chemical oxidation of iron(III) porphyrins have been designed in order to elucidate structure and reactivities of the higher valent iron porphyrin species. Eminent among these are the studies of Balch[2] and Groves[3] which have dealt with investigations of iron(IV)–oxo porphyrins (peroxidase compound II model) and an investigation of Balch[2c] which provides evidence for an iron(IV)–oxo porphyrin π-cation radical (peroxidase compound I model). Electrochemistry has not been vigorously pursued as a means to both generate and to determine oxidation potentials of iron(IV)–oxo porphyrins and iron(IV)–oxo porphyrin π-cation radicals. We now report the spectral and electrochemical characterization of an electrochemically generated iron(IV)–oxo porphyrin and an iron(IV)–oxo porphyrin π-cation radical.

It is now accepted that the first $1e^-$ oxidation of an iron(III) porphyrin ligated to such anions as Cl^-, ClO_4^-, etc. is porphyrin centered resulting in the formation of an iron(III) porphyrin π-cation radical. Further $1e^-$ oxidation leads to an iron(III) porphyrin dication.[5] These electrochemical studies did not include strongly basic oxyanions as ligands due to the problem of μ-oxo-dimer formation. We have examined the electrochemistry of sterically hindered porphinato iron(III) hydroxide and methoxide salts and have demonstrated that the ligation of strongly basic oxy ligands results in a new peak. The presence of this new peak (about 100 mV less positive than the first oxidation for the chloride salt of the corresponding iron(III) porphyrin) was taken as the first evidence for the room-temperature existence of iron(IV)–oxo species; however, this species is only stable at ambient

(1) (a) Morrison, M.; Schonbaum, G. R. *Annu. Rev. Biochem.* **1976**, *45*, 861. (b) Hewson, W. D.; Hager, L. P. In "The Porphyrins"; Dolphin, D., Ed.; Academic Press: New York, 1979; Vol. VII; pp 295–332. (c) Dunford, H. B.; Stillman, J. S. *Coord. Chem. Rev.* **1976**, *19*, 187. (d) Theorell, H. *Enzymologia* **1941**, *10*, 250. (f) Dolphin, D.; Forman, A.; Borg, D. C.; Fajer, J.; Felton, R. H. *Proc. Natl. Sci. U.S.A.* **1971**, *68*, 614. (f) Groves, J. T. *Adv. Inorg. Biochem.* **1979**, 119. (g) Hayashik, Y.; Yamazaki, I. *J. Biol. Chem.* **1979**, *154*, 9101.
(2) (a) Balch, A. L.; Chan, Y. W.; Cheng, R. J.; LaMar, G. N.; Latos-Grazynski, L.; Renner, M. W. *J. Am. Chem. Soc.* **1984**, *106*, 7779. (b) Chin, D. H.; Balch, A. L.; LaMar, G. N.; Balch, A. L. *J. Am. Chem. Soc.* **1980**, *102*, 4344. (c) Balch, A. L.; Latos-Grazynski, L.; Renner, M. W. *J. Am. Chem. Soc.* **1985**, *107*, 2983.
(3) (a) Groves, J. T.; Quinn, R.; McMurry, T. J.; Nakamura, M.; Lang, G.; Boso, B. *J. Am. Chem. Soc.* **1985**, *107*, 354. (b) Groves, J. T.; Nemo, T. E. *J. Am. Chem. Soc.* **1983**, *105*, 5786. (c) Groves, J. T.; Myers, R. S. *J. Am. Chem. Soc.* **1983**, *105*, 5791.
(4) Lee, W. A.; Calderwood, T. S.; Bruice, T. C. *Proc. Natl. Sci. U.S.A.* **1985**, *82*, 4301.
(5) (a) Phillippi, M. A.; Shimomura, E. T.; Goff, H. M. *Inorg. Chem.* **1981**, *20*, 1322. (b) Phillippi, M. A.; Goff, H. M. *J. Am. Chem. Soc.* **1982**, *104*, 6026.

Figure 1. Visible spectra (at −78 °C) of the *meso*-tetrakis[(2,4,6-trimethylphenyl)porphinato]iron(IV) hydroxide species ([(TMP)-Fe^{IV}OH]$^+$) formed by $1e^-$ oxidation of (TMP)Fe^{III}OH and the corresponding iron(IV) hydroxy porphyrin π-cation radical ([·(TMP)-Fe^{IV}OH]$^{2+}$) formed by $1e^-$ oxidation of ([TMPFe^{IV}OH]$^+$) in 5% CH$_3$OH/CH$_2$Cl$_2$ (with 0.1 M tetrabutylammonium perchlorate). From repetitive spectral scanning isosbestic points for oxidation of TMPFe^{III}OH to [TMPFe^{IV}OH]$^+$ were determined to be at 405, 425, 502, and 550 nm while the maximum absorbances of the latter are found at 415 (Soret band) and 525 nm. For [·(TMP)Fe^{IV}OH]$^{2+}$ isosbestic points are at 400, 426, 485, and 545 nm while maximum absorbances of the latter are found at 398, 412, 600, and 670 nm. With the exception of a small bathochromic shift of approximately 5 nm in the α,β region, the spectrum shown in this figure are unaltered on transfer to Burdick and Jackson dichloromethane solvent.

temperatures on the cyclic voltammetric time scale (scan rate = 25–400 mV/s).[4]

In order to observe the iron(IV)–oxo porphyrin products of the electrochemical oxidation a special 1.0-mm spectroelectrochemical quartz cuvette was designed with a gold minigrid (10^3 lines/in.^{2}) working electrode; in quartz side compartments fused to the cuvette a platinum flag auxiliary electrode (separated from the cuvette by a medium glass frit) and an Ag/AgCl reference electrode (filled with aqueous tetramethylammonium chloride, adjusted to 0.00 V vs. saturated calomel electrode) were mounted. The entire apparatus was maintained at −78 °C. For the purpose of the present study *meso*-tetrakis[(2,4,6-trimethylphenyl)porphinato]iron(III) hydroxide [(TMP)Fe^{III}OH] was used as the representative iron(III) porphyrin. The solvent employed was CH$_2$Cl$_2$ (Burdick and Jackson). Potentials for consecutive $1e^-$ oxidation of (TMP)Fe^{III}OH were determined by conventional CV at −78 °C. Oxidation products were generated in the spectroelectrochemical cuvette by $1e^-$ and $2e^-$ controlled-potential electrolysis at the required potentials. Constant monitoring of the visible spectra was carried out during the course of the electrochemical oxidations. In Figure 1 there are presented the visible spectra of (TMP)Fe^{III}OH and its 1- and 2e^- oxidation products. Examination of Figure 1 shows that the first $1e^-$ oxidation (1.05 V vs. SCE) results in a decrease in absorbance of the Soret band (415 nm) without a change in its position and a new absorption peak appears at 520 nm. The latter is not associated with the starting (TMP)Fe^{III}OH nor to the eventual decomposition product [(TMP)Fe^{III}Cl] of the electrochemical reaction. The π-cation radical of (TMP)Fe^{III}Cl also displays an absorbance around 520 nm; on the other hand the most characteristic feature for the visible spectrum of a π-cation radical is the shift of the Soret band to below 400 nm.[3] This is clearly not observed during the $1e^-$ oxidation of (TMP)Fe^{III}OH. Additional evidence that the product is [(TMP)Fe^{IV}OH]$^+$ was obtained by the addition of 1 equiv of 1-methylimidazole which brought about a shift of the 520-nm peak to 570 nm, which is consistent with Balch's report of an absorbance at 560 nm (toluene) of iron(IV) *meso*-tetraphenylporphyrin ligated to 1-methylimidazole.[2b] The λ_{max} values of [(TMP)Fe^{IV}OH]$^+$ and [(TMP)Fe^{IV}OCH$_3$]$^+$ in 5% CH$_3$OH/CH$_2$Cl$_2$ (v/v) are at 525 nm. On addition of 1 equiv of CH$_3$O$^-$ to the electrochemically